



## High spatial resolution solar-induced chlorophyll fluorescence and its relation to rainfall precipitation across Brazilian ecosystems

Luis Miguel da Costa <sup>a,\*</sup>, Gislaine Costa de Mendonça <sup>a</sup>, Gustavo André de Araújo Santos <sup>b,c</sup>, José Reinaldo da Silva Cabral de Moraes <sup>a</sup>, Roberto Colombo <sup>d</sup>, Alan Rodrigo Panosso <sup>a</sup>, Newton La Scala Jr. <sup>a</sup>

<sup>a</sup> Department of Engineering and Exact Sciences, São Paulo State University Faculty of Agrarian and Veterinary Sciences (FCAV-UNESP), Via de Acesso Prof. Paulo Donato Castellane s/n, 14884-900, Jaboticabal, São Paulo, Brazil

<sup>b</sup> Advanced Campus Porto Franco, Federal Institute of Education, Science and Technology of Maranhão – IFMA, Rua Custódio Barbosa, no 09, Centro, Porto Franco, Maranhão, 65970-000, Brazil

<sup>c</sup> Center of Agricultural, Natural and Literary Sciences, State University of the Tocantins Region of Maranhão (UEMASUL), Av. Brejo do Pinto, S/N – Brejo do Pinto, Estreito, Maranhão, 65975-000, Brazil

<sup>d</sup> Remote Sensing of Environmental Dynamics Lab., DISAT, University of Milano-Bicocca, P.zza della Scienza 1, 20126, Milano, Italy

### ARTICLE INFO

#### Keywords:

Remote sensing  
Biome sensitivity  
Photosynthesis  
Physiognomic diversity

### ABSTRACT

The detection of Solar-Induced chlorophyll Fluorescence (SIF) by remote sensing has opened new perspectives on ecosystem studies and other related aspects such as photosynthesis. In general, fluorescence high-resolution studies were limited to proximal sensors, but new approaches were developed to improve SIF resolution by combining OCO-2 with MODIS orbital observations, improving its resolution from 0.5° to 0.05 on a global scale. Using a high-resolution dataset and rainfall data some SIF characteristics of the satellite were studied based across 06 contrasting ecosystems in Brazil: Amazonia, Caatinga, Cerrado, Atlantic Forest, Pampa, and Pantanal, from years 2015–2018. SIF spatial variability in each biome presented significant spatial variability structures with high  $R^2$  values ( $>0.6$ , Gaussian models) in all studied years. The rainfall maps were positively and similar related to SIF spatial distribution and were able to explain more than 40% of SIF's spatial variability. The Amazon biome presented the higher SIF values ( $>0.4 \text{ W m}^{-2} \text{ sr}^{-1} \mu\text{m}^{-1}$ ) and also the higher annual rainfall precipitation (around 2000 mm), while Caatinga had the lowest SIF values and precipitations ( $<0.1 \text{ W m}^{-2} \text{ sr}^{-1} \mu\text{m}^{-1}$ , precipitation around 500 mm). The linear relationship of SIF to rainfall across biomes was mostly significant (except in Pantanal) and presented contrasting sensitivities as in Caatinga SIF was mostly affected while in the Amazon, SIF was lesser affected by precipitation events. We believe that the features presented here indicate that SIF could be highly affected by rainfall precipitation changes in some Brazilian biomes. Combining rainfall with SIF allowed us to detect the differences and similarities across Brazil's biomes improving our understanding on how these ecosystems could be affected by climate change and severe weather conditions.

### 1. Introduction

Space and time remote monitoring of vegetation in tropical ecosystems is fundamental to better understanding of the terrestrial cycle over different perspectives, such as, water cycle (Cui et al., 2018), energy (Liang et al., 2019) and carbon cycles (Xiao et al., 2019). Considering this, photosynthesis plays an important role in this cycle and is quite dependent on climatic conditions such as temperature and precipitation

(Barbosa et al., 2015), or with radiation (Uribe et al., 2021; da Costa et al., 2022), but it is also related to the plant's physiology. For example, C3 plants are more sensitive to temperature changes than C4 and CAM plants (Ainsworth and Long, 2005; Turner et al., 2021), and canopy structure, such as age and height, where tall and old trees are more resilient to environmental conditions (Giardina et al., 2018; Pinagé et al., 2022).

Recently Solar-Induced chlorophyll Fluorescence (SIF) has been used

\* Corresponding author.

E-mail addresses: lm.costa@unesp.br (L.M. da Costa), gislaine.cmendonca@gmail.com (G.C. de Mendonça), gustavo\_anndre@hotmail.com (G.A. Araújo Santos), reinaldojmoraes@gmail.com (J.R.S.C. Moraes), roberto.colombo@unimib.it (R. Colombo), alan.panosso@unesp.br (A.R. Panosso), la.scala@unesp.br (N. La Scala Jr.).

as a proxy for photosynthesis as it captures the chlorophyll-a re-emission of photons absorbed by the plant, which occurs at any stage of its development between the wavelength of ~650 nm–~800 nm (Sun et al., 2018; Mohammed et al., 2019). The detection of SIF in different scales (Cogliati et al., 2019; Siegmann et al., 2021; Doughty et al., 2022) has opened a new perspective for understanding the carbon uptake (Hao et al., 2021; Martini et al., 2022), drought effects (Sun et al., 2020; Qiu et al., 2022), and ecology (Tagliabue et al., 2019), in several ecosystems (Parazoo et al., 2013; Guan et al., 2016; Araújo Santos et al., 2022).

In general, space missions that monitor SIF have certain limits concerning the retrieval of the full spectrum of fluorescence due to atmospheric corrections and the reabsorption process in the red region (~685 nm) of the spectrum respectively (Cogliati et al., 2019; Mohammed et al., 2019; Romero et al., 2020). Alternatively, the retrieval algorithms for space missions generally focus on the far-red region (~740 nm) due to the band overlap that occurs between the O<sub>2</sub> column wavelength and those emitted by chlorophyll in far-red (Celesti et al., 2018; Sun et al., 2018), such as for Orbiting Carbon Observatory 2 (OCO-2) that retrieve SIF at 757 nm and 771 nm (Crisp et al., 2017).

Another limitation of remote sensing of SIF is the spatial resolution, which until 2016 was 0.5°–1.0° (Yu et al., 2019a). With the launch of TROPOspheric Monitoring Instrument (TROPOMI), this resolution was refined to 0.1° (Quanter et al., 2015, 2021); however, the other satellites have more orbit time, given this, the improvement of their spatial resolution was necessary. One of the first frameworks developed to improve this spatial resolution was performed by Duveiller and Cescatti (2016), who developed an empirical framework with 0.05° resolution using MODIS spectral reflectance and GOME-SIF data. This and other study models have a common point: the use of other remote sensing products, mainly vegetation indices, to improve SIFs spatial resolution (Duveiller and Cescatti, 2016; Zhang et al., 2018; Li and Xiao, 2019; Yu et al., 2019a).

Given the importance of Tropical ecosystems both for diversity and global primary production (34%–40%) where the Brazilian Amazon biome stores about 10% of the global forest carbon (Salunkhe et al., 2018; Raha et al., 2020; Heinrich et al., 2021), some studies have been performed in the Amazonian ecosystem to exploit the XCO<sub>2</sub>-SIF relationship, reporting an inverse correlation between these variables (Parazoo et al., 2013; Albright et al., 2022). Additionally, these researches study phenological diversity and drought effects over the Amazon (Castro et al., 2020), or drought effects in the Brazilian Caatinga (Bontempo et al., 2020).

In tropical ecosystems the temperature is not the most relevant aspect for vegetation cover, as shown by Xu et al. (2018). That study observed that the sensitivity and importance of annual mean precipitation are higher in these regions, and reported that the rainfall variability is also relevant across space. Following this, more recently, Besnard et al. (2021) also report that rainfall is more important in tropical ecosystems than temperature and, in addition, they also show that in a semi-arid environment the sensitivity is higher as well the importance, compared to the forest covers.

Additionally, structure differences between the vegetation cover imply a different response to environmental conditions as more complex vegetation has more resilience (Köhler et al., 2018; Pinagé et al., 2022), as well the root system of the tallest and oldest vegetation enables more resilience for the plants (Giardina et al., 2018). Given this, in this study we applied a geospatial approach to study SIF signal across Brazilian biomes and relate it to climate aspects like precipitation along Brazilian territory.

## 2. Materials and methods

### 2.1. Study area

The study was conducted in Brazil ( $\approx 8.5 \times 10^6 \text{ km}^2$ ), a territory

characterized mostly as tropical (81%), partly by humid subtropical (14%) climate, and semi-arid (5%), with microclimatic variations, according to the Koppen classification (Alvares et al., 2013). The Brazilian territory is delimited by a natural macro division: the biomes, subunit grids of the biosphere characterized and grouped by a series of functional and structural characteristics, particularly morphoclimatic and phytogeographic, which encompass different types of communities (animal/vegetal), habitats, and ecosystems.

On a continental scale, there are six characteristic biomes: i) Amazon (AMZ), having an average annual precipitation of 2200 mm; ii) Cerrado (CER) (savanna), with annual precipitation of 1400 mm; iii) Caatinga (CAAT), having an average annual precipitation of around 640 mm; iv) Atlantic Forest (ATF), having an annual precipitation of around 1400 mm; v) Pampa (PMP), also with an average annual precipitation around 1400 mm and vi) Pantanal (PNT) with a precipitation around 1145 mm (Zappi et al., 2015; Paredes-Trejo et al., 2019) (Fig. 1).

The Amazon, Pantanal, and almost the entire Cerrado are classified as tropical, while the Atlantic Forest has some part classified as tropical, especially in the coast and in the regions close to the Cerrado. The other part, closer to the south, is classified as humid subtropical zone. Pampa biome is classified as humid subtropical, and finally the Caatinga is mainly characterized by the semi-arid dry zone, with some areas that are composed by the tropical zone with dry winter, especially in the transition between Caatinga and Cerrado and the Atlantic Forest (Alvares et al., 2013).

### 2.2. High spatial resolution solar-induced chlorophyll fluorescence from satellite observations

For this work, the first version of the database described by Yu et al. (2019a) available in the NASA repository (Yu et al., 2019b) was used. This dataset constitutes a model built from a combination of SIF at 757 nm and 771 nm data obtained in the Orbiting Carbon Observatory 2 (OCO-2; Crisp et al., 2012; O'Dell et al., 2012) and by NDVI data from the MODIS sensors (Huete et al., 2002) to ensure better spatial resolution. Overall, the strategy consists in using a neural artificial network to train the OCO-2 SIF against the MODIS bidirectional reflectance that are co-located with the OCO-2 footprint, then the model to predict the gaps of SIF is applied using as predictor the contiguous measurements of MODIS. In addition, to evaluate the model, the authors performed a validation with a proximal SIF sensor where the adjusted coefficient of determination was above 0.7 ( $p < 0.001$ ; Yu et al., 2019a).

#### 2.2.1. SIF pre-processing

The steps involved from data acquisition to the generation of the end result consist of four steps: I) The acquisition of data through the NASA repository (Yu et al., 2019b) where biweekly files for the entire world are found, for years 2015–2018. II) The entire process of filtering the data, delimiting the region of interest, filtering outliers and then aggregating annual averages for each coordinate was performed in the R programming language and is available on Github ([https://github.com/lm-costa/Sif\\_005\\_br](https://github.com/lm-costa/Sif_005_br)). III) A new dataset consisting in 4 files for the Brazilian territory was created, each file has an aggregation by year of the SIF values, thus facilitating the access for the general community, and IV) the formal analysis, with the descriptive statistic, Tukey test, and geostatistical modeling by ordinary kriging (OK).

### 2.3. Rainfall data

Daily precipitation along the country was obtained from the National Aeronautics and Space Administration/World Energy Resources Forecasting Platform (NASA/POWER) and was evaluated as annual averages for the entire Brazilian territory. This platform provides data with a resolution of 1° (Stackhouse et al., 2015). Other recent studies such as Morais Filho et al. (2021) and da Costa et al. (2021) have related SIF and XCO<sub>2</sub> data obtained from OCO-2 with meteorological data such as the

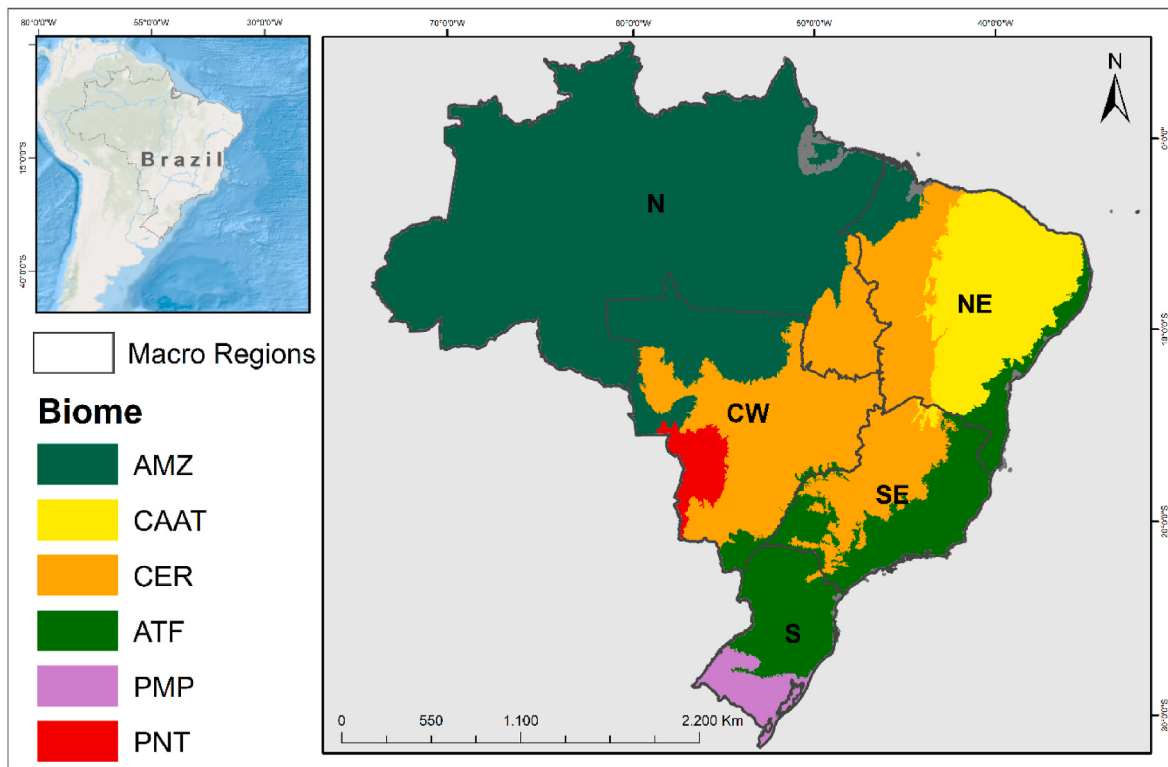


**Fig. 1.** Study area and Brazilian Ecosystem division. The inset image shows Brazil's administrative regions.

ones obtained in NASA/POWER.

#### 2.4. Mapping SIF by ordinary kriging (O.K)

Ordinary kriging (O.K) is the most applied geostatistical method of interpolation of georeferenced data, being applied in several studies such as spatial distribution of soil carbon stock (Freitas et al., 2018; Terçariol et al., 2016; Panosso et al., 2009), the spatial distribution of NDVI, and other vegetation indices (Siabi et al., 2019; Falahatkar et al., 2017; Yang et al., 2011), including studies conducted with SIF (Tadić et al., 2015; Tadić et al., 2017).

In this work, this analysis was applied to identify the different typologies across the Brazilian biomes using SIF signal and was performed in ArcGIS software by fitting the experimental variogram, based on the intrinsic hypothesis proposed by Isaaks and Srivastava (1989), where the variogram describes the spatial continuity of the variables as a function of the distances between two locations, being estimated by equation (1) (Eq (1)):

$$\hat{\gamma}(h) = \frac{1}{2N(h)} \times \sum_{i=1}^{N(h)} [z(x_i) - z(x_i + h)]^2 \quad (1)$$

Where,  $\hat{\gamma}(h)$  is the experimental semivariance for a separation distance  $h$ ,  $z(x_i)$  is the property value of SIF at point  $i$ , and  $N(h)$  is the number of pairs of points separated by distance  $h$ . During the modeling of the experimental variogram, the model coefficients are estimated: nugget effect ( $C_0$ ), sill ( $C_0+C_1$ ), and range ( $A$ ).

The choice between the best-fitted model was made through cross-validation where linear regression is performed between the values estimated by the semivariogram and the observed values (Panosso et al., 2009; Terçariol et al., 2016). In our study, the best geostatistical model was the Gaussian model for all cases (Eq. (2)). More details can be found in the supplementary material.

$$\hat{\gamma}(h) = C_0 + C_1 \left\{ 1 - \exp \left[ -3 \left( \frac{h}{a} \right)^2 \right] \right\}, 0 < h < d \quad (2)$$

where  $d$ : is the maximum distance that the variogram is defined.

#### 2.5. Statistical analysis

The SIF dataset was aggregated as an annual mean for each coordinate, then a descriptive statistic was applied and also submitted to a Tukey test with 5% of significance to evaluate the differences across the Brazilian biomes presented in Fig. 1. A simple linear regression between SIF and Rainfall observations was employed, which is collocated in the whole country and across the ecosystems to identify the SIF response to this variable and the sensitiveness (slope) of each Brazilian biome.

### 3. Results

SIF distribution maps presented in Fig. 2 indicate high spatial variability throughout the country with values lower than 0.1 to as high as  $0.41 \text{ W m}^{-2} \mu\text{m}^{-1} \text{ sr}^{-1}$ . In all years, the North region presented the higher values and this is where the Amazon biome is located. Conversely, the Northeast region presents the lowest values, especially due to the Caatinga ecosystem. In the Central-South regions, intermediate values of SIF values were observed with some hot spots located in Atlantic Forest biome. Despite following a very similar pattern from 2015 to 2018, fluctuations are noticeable in the same biome along the years, especially in CAAT environment which also presented lower and higher SIF values in 2015 and 2018, respectively (also seen in Fig. 2).

Fig. 3 presents the mean values of SIF across Brazilian biomes along the studied years. Higher values were observed in the Amazon (AMZ) biome with values as high as  $0.34 \pm 0.045$  and  $0.36 \pm 0.043 \text{ W m}^{-2} \mu\text{m}^{-1} \text{ sr}^{-1}$  for years 2016, 2018, and 2017, respectively. In one of the years (2017) the Atlantic Forest (ATF) presented values closer to AMZ  $0.32 \pm 0.060 \text{ W m}^{-2} \mu\text{m}^{-1} \text{ sr}^{-1}$ . On the other hand, lower SIF values

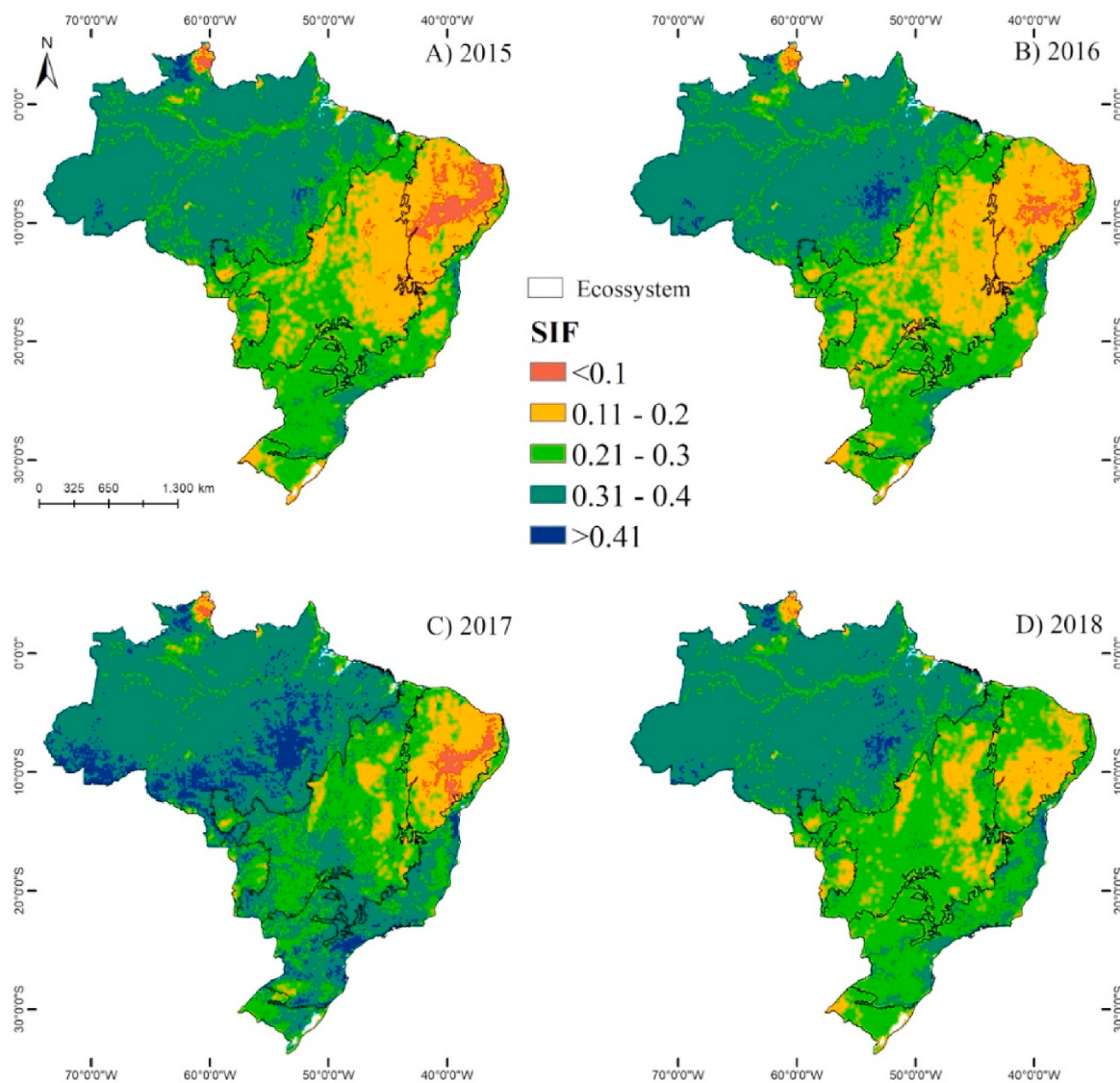


**Fig. 2.** Annual variability of High-Resolution SIF over Brazilian biomes between 2015 and 2018.

were observed in the Caatinga biome (CAAT) with averages as low as  $0.13 \pm 0.050 \text{ W m}^{-2} \mu\text{m}^{-1} \text{ sr}^{-1}$  in 2015. It is noticeable that SIF means in CAAT increased over the years getting closer to the other biomes (Cerrado (CER), Pampa (PMP), and Pantanal (PNT)) with intermediate SIFs between  $0.20$  and  $0.28 \text{ W m}^{-2} \mu\text{m}^{-1} \text{ sr}^{-1}$ . In the year 2017, those last 03 biomes presented higher mean values between  $0.28$  and  $0.31 \text{ W m}^{-2} \mu\text{m}^{-1} \text{ sr}^{-1}$ . Low values outliers were mostly observed in AMZ for all the studied years.

Comparing Brazilian biomes (Fig. 1) with SIF mean values, maps (Figs. 2 and 3) show extremes in Amazonia and Caatinga environments, with higher and lower values, respectively. But among Cerrado, Pantanal, Pampa, and the Atlantic Forest biomes presented similar SIFs with some years presenting spots with closer AMZ and CAAT values. Tukey test (inset Fig. 3, p-value <0.05) confirms that Amazon biome had higher mean values when compared to the others, while Caatinga presented the lower values with the other biomes in between those.

In order to better understand the means and variability observed in SIF data, Fig. 4 presents rainfall precipitation along the country. Higher precipitations were observed in AMZ biome during the studied years while lower precipitations were observed in CAAT. In other biomes the amount of precipitation was intermediary.

The interannual/spatial variability of rainfall in Brazil is extreme,

especially comparing the North to South regions. In the Northeast region (predominance of the Caatinga Biome), the accumulated annual rainfall could be less than 500 mm, as in 2015, which was the driest year in that region (Fig. 4). In contrast, the North region (predominance of the Amazon Biome) presented the highest concentrations of rainfall in some locations and years exceeding 3000 mm. However, in this same region, annual averages could be as low as 500 mm, close to those observed in CAAT.

In the Midwest and Southeast Regions where the Cerrado, Pantanal, and the Atlantic Forest Biomes prevail, rainfall between 1000 and 1500 mm is observed. Finally, in the southern region, the Pampa grasslands, and portions of the Atlantic Forest, rainfall between 1500 and 2000 mm is noticed, except for 2018 when it had lower values for this region. In general, higher and lower spots in precipitation maps are similarly located where higher hot and cold spots in SIF were noted.

In order to relate SIF with rainfall precipitations, a linear correlation analysis crossing both variables along the studied ecosystems (Fig. 5 and Table 1) was used. In general, precipitation explains about 45% of the variability of SIF in Brazil (Supplementary Fig. 4), having a growth rate of  $+0.0001 \text{ W m}^{-2} \text{ sr}^{-1} \mu\text{m}^{-1}$  for each mm of rainfall. However, the specific relations in each biome are different, as seen in Fig. 5 and Table 1. Except for the Pantanal biome, all the other biomes presented

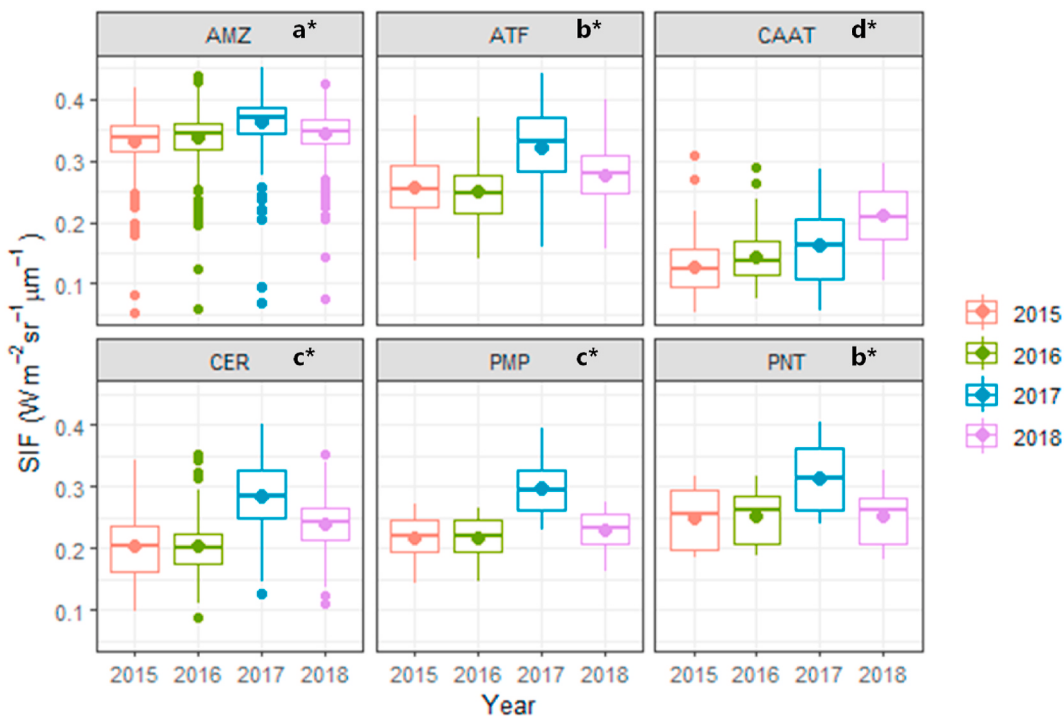


**Fig. 3.** Annual mean and deviation for the High-Resolution Solar-Induced chlorophyll Fluorescence (SIF ( $\text{W m}^{-2} \mu\text{m}^{-1} \text{sr}^{-1}$ )) in studied years and ecosystems in Brazil. Small inset letters represent the result of Tukey test ( $p\text{-value} < 0.05$ ).

significant relations between SIF and annual rainfall precipitation in the four-year studied period. One important aspect is related to the derivative (sensitivity) of SIF in relation to rainfall in each of the biomes, which presented contrasting values as high as  $1.87\text{e-}04 \text{ W m}^{-2} \text{sr}^{-1} \mu\text{m}^{-1} \text{mm}^{-1}$  to as low as  $8.71\text{e-}06 \text{ W m}^{-2} \text{sr}^{-1} \mu\text{m}^{-1} \text{mm}^{-1}$  in CAAT and AMZ.

Contrasting responses of SIF to rainfall were observed, with the most sensitive biome being the Caatinga, with a slope (b coefficient) 100 times higher than observed in the Amazon biome and around 10 times higher when compared to the other biomes. The linear correlation coefficient (r) shows better correlation in CAAT ecosystem between the SIF and Rainfall ( $r = 0.63$ ), followed by Pampa ( $r = 0.38$ ) and Cerrado ( $r = 0.34$ ). Although the Amazon and the Atlantic Forest don't have the best correlations values, the regression significance was less than 0.001. However, the Pantanal does not have a significant regression between SIF and Rainfall.

#### 4. Discussion

##### 4.1. SIF space and time patterns

Regarding the spatial distribution of the studied data and comparing SIF variability for Brazil with global studies (Tadić et al., 2015; Tadić et al., 2017; Zhang et al., 2018; Yu et al., 2019a; Li and Xiao, 2019) our results show similar patterns for all years having similar ranges (means between  $0 < \text{SIF} < 0.4$ ). Small changes were noted in SIF spatial distributions considering years 2015–2018. When aggregated in year, this is an important aspect as it shows a specific pattern for each biome according to its characteristic vegetation and climate condition (Zappi et al., 2015) indicating that SIF could be applied to large ecosystems studies (Frankenberg and Berry, 2018).

The spatial patterns of SIF (Fig. 2) exhibited a similar gradient from North to South over the years and showed a consistent response to the biome and precipitation types that extend latitudinally across the country. The vegetation typology and climate predominant in the Amazon and semi-arid regions allowed for a sharper detection of these

physiographic domains. This is evident in the analysis of the averages for each biome (Fig. 3) where for all years the Amazon ecosystem presents the highest SIF values and the Caatinga the lowest, following an intermediate gradient composed of the Atlantic Forest, Cerrado, Pantanal, and Pampa regions.

This could be related to the fact that forests that have reached climax are at the most mature stage of ecological succession, and growth rates and biomass production is self-perpetuating and constant, in contrast to transient communities such as crops (Odum, 1971; Du and de Vries, 2018; Anderegg et al., 2020; Gora and Esquivel-Muelbert, 2021). On the other hand, Caatinga with low SIF is distributed in semi-arid regions with low precipitation, limiting the photosynthesis (Silva and Cruz, 2018). In addition, since crops have seasonal growth, this also impacts the space-time variability of SIF (Siabi et al., 2019; Moraes Filho et al., 2021; da Costa et al., 2021).

Merrick et al. (2019), presented the same difficulty in differentiating low-resolution SIF interannual averages of Atlantic Forest, Pampa, Cerrado, and Pantanal when studying the interannual differences of SIF in the Brazilian biomes but not considering the spatial variability, the same observed in our study. They identified that the annual averages for the Amazon are the highest and conversely Caatinga presents the lowest annual averages.

It is noteworthy that even in forest habitats as in the Amazon biome, phytogeographical variations of the forest (Tuomisto et al., 1995) can be found with the highest SIF values ( $>0.41 \text{ W m}^{-2} \text{sr}^{-1} \mu\text{m}^{-1}$ ) usually in locations having dense Ombrophylous Forest formations (INPE, 2008). In addition to the vegetative gradients of dense forests the composition and structure of the rainforest in the Amazon basin presents floodplains (igapó) composed by herbaceous and aquatic vegetation that are related to the regulation of the flood pulses of Amazonian rivers (Oliveira-Filho et al., 2021) which explains the SIF range from  $0.21$  to  $0.30 \text{ W m}^{-2} \text{sr}^{-1} \mu\text{m}^{-1}$  over the hydrographic conformations, making its identification possible in contrast to other ecosystems.

Additionally, the new Amazonian agricultural border in the south of the Amazonian region and eastern of Mato Grosso and Pará states may also explain the SIF values typically varying from  $0.21$  to  $0.3 \text{ W m}^{-2} \text{sr}^{-1}$

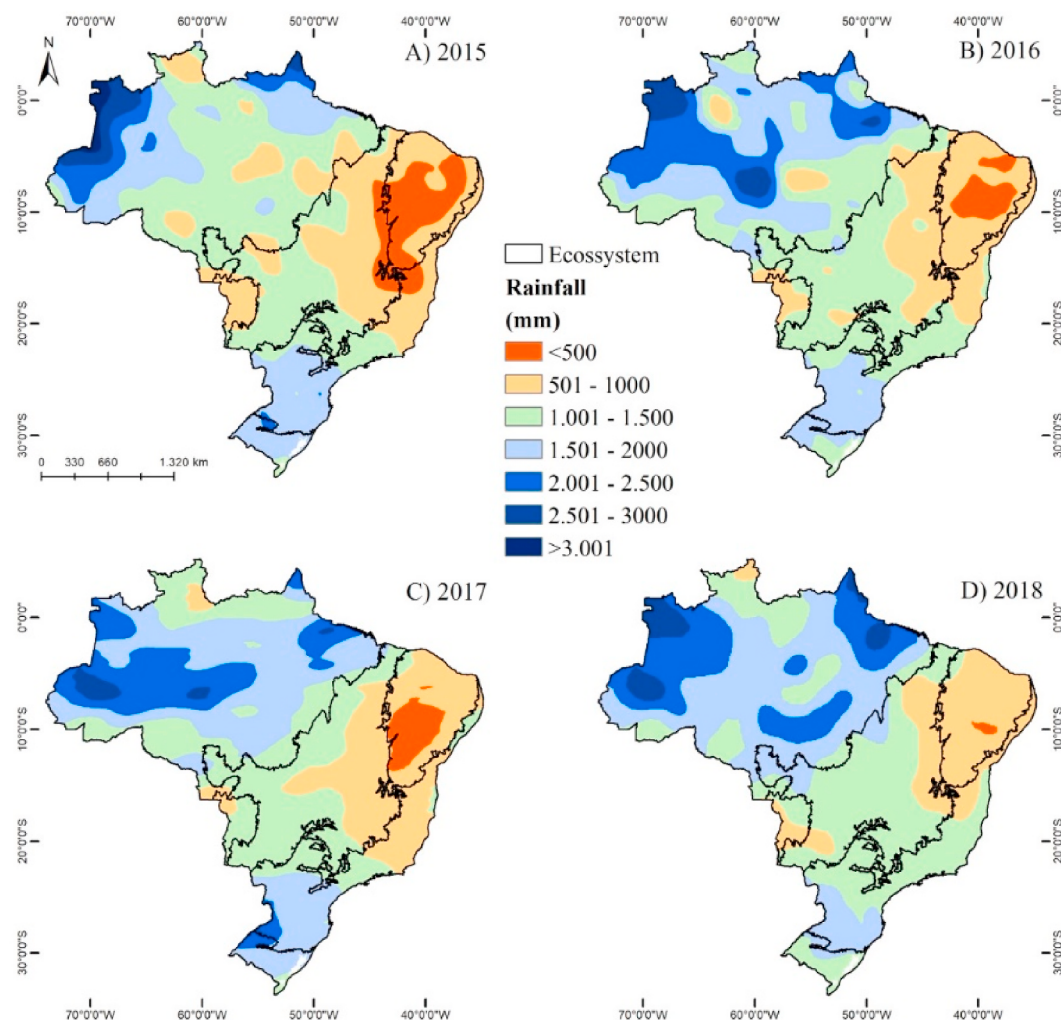


**Fig. 4.** Annual variability of Rainfall over Brazilian biomes between 2015 and 2018.

$\mu\text{m}^{-1}$ , where vast areas with soybean and cotton cultivation including pasture lands have been established (Silva Junior and Lima, 2018; Barbosa et al., 2021). Similar to those observed in the Amazon region, high SIF values ( $>0.31 \text{ W m}^{-2} \text{ sr}^{-1} \mu\text{m}^{-1}$ ) also extend as spaced patches in the coastal strips and in the central and southeastern regions of the country, which converge with foci of remnant vegetation of the Atlantic Forest biome (Parras et al., 2020).

The Atlantic Rainforest is one of the world's biodiversity hotspots and the second largest tropical rainforest on the American continent with a heterogeneous forest formation (Myers et al., 2000; Câmara, 2003; SOS Mata Atlântica & INPE, 2017). Additionally, it presents a significant variation in its net primary productivity with increments at the beginning of the rainy season (Santos et al., 2021), reflecting in the interannual variation of SIF in the order of  $0.31\text{--}0.4 \text{ W m}^{-2} \text{ sr}^{-1} \mu\text{m}^{-1}$ . However, the variability of SIF when compared with the original limits of the Atlantic Forest Biome shows the intense degree of deforestation in this region caused by centenarian loss of native vegetation and conversion to agricultural land (Morellato and Haddad, 2000), which has varied phenological and photosynthetic behavior throughout the year and consequently influence the SIF spatial pattern.

Currently, the Atlantic Forest and Cerrado are the most anthropogenic regions of Brazil with the largest agricultural areas in the country (Bordonal et al., 2018; de Mendonça et al., 2022) and despite the diversity of commercial species and soil covers, the photosynthetic activity of the main Brazilian crops (sugarcane and soybean) is similar, as they are from the same plant family Poaceae (Judd et al., 2009; Evert and

Eichhiri, 2014). Given this, the phytobiognomic differentiation of those biomes is incipient, highlighting only the presence of Atlantic Forest remnants, native or reforested, differentiating those from agricultural lands through the visualization of scattered green patches in the cartographic delimitation biome (Morellato and Haddad, 2000; Parras et al., 2020; de Mendonça et al., 2022).

#### 4.2. The relation between SIF and precipitation

Paredes-Trejo et al. (2019) investigated the annual rainfall distribution in each Brazilian biome and concluded that the Amazon (2200 mm) has a total almost twice as large as the Atlantic Forest (1457 mm), Pampa (1433 mm), Pantanal (1145 mm) and Cerrado (1400 mm), and more than 3 times larger than Caatinga (639 mm) going in agreement with the results presented in our study. Overall, the precipitation explains more than 40% of annual SIF variability (Supplementary Fig. 4), and the spatial variability patterns and relationships of SIF with rainfall follow the average annual rainfall volume for each biome resulting in higher plant fluorescence (Fig. 2 and 4).

The relationship between SIF and precipitation was also investigated in CONUS (Turner et al., 2021) highlighting high rates of SIF and GPP distributed mainly in forest and savanna biomes with sufficient precipitation, while scrub and grassland biomes with low SIF and GPP were distributed mainly in regions having low precipitation, and although scrubs and grassland had low SIF values these ecosystems have a higher SIF sensitivity to precipitation as well as in Caatinga compared to the

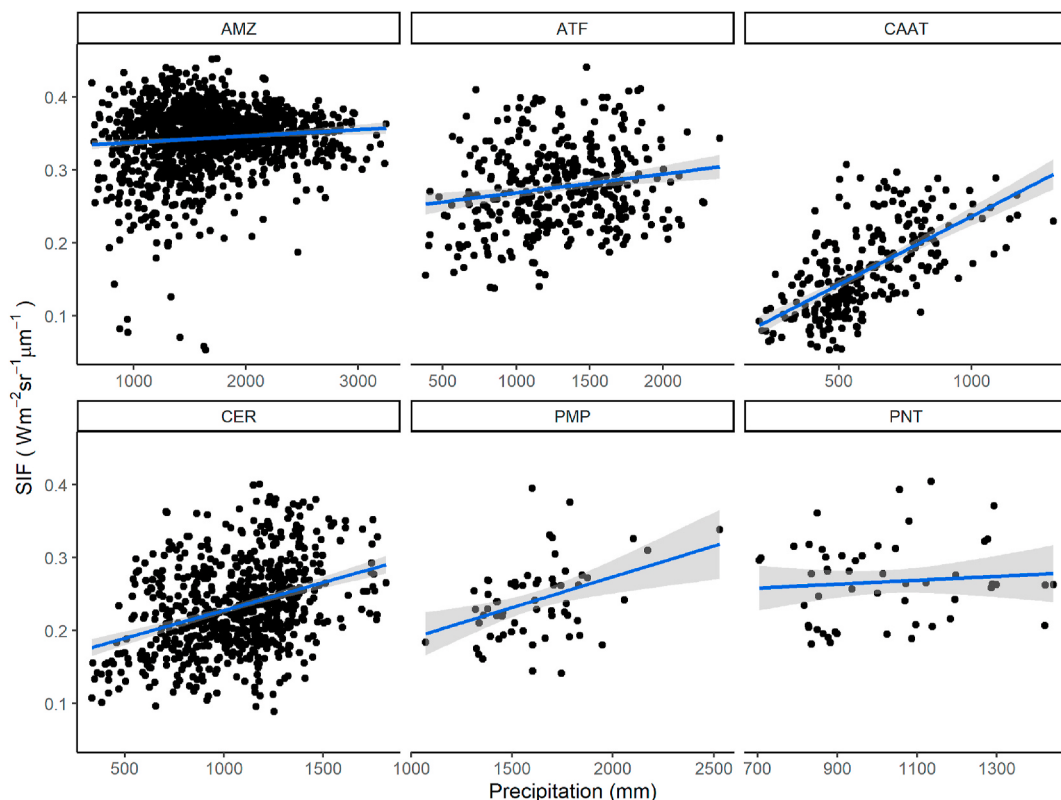


**Fig. 5.** Linear regressions between SIF and rainfall along ecosystems.

**Table 1**

Summary coefficients of the linear regression between SIF and Rainfall and the respective statistics across Brazilian Biomes. Where:  $a$  is the linear coefficient in  $\text{W m}^{-2} \text{sr}^{-1} \mu\text{m}^{-1}$ ;  $b$  is the slope/sensitiveness in  $\text{W m}^{-2} \text{sr}^{-1} \mu\text{m}^{-1} \text{mm}^{-1}$ ;  $r$  = Pearson's linear correlation coefficient and  $N$  is the number of observations.

Biome	$SIF = a + b \times Rainfall$				
	$a$	$b$	p-value	R	N
Amazon	3.29e-01	8.71e-06	<0.001	0.10	1316
Atlantic Forest	2.43e-01	2.55e-05	<0.001	0.17	388
Cerrado	1.52e-01	7.64e-05	<0.001	0.34	688
Caatinga	4.96e-02	1.87e-04	<0.001	0.63	260
Pampa	1.06e-01	8.41e-05	<0.001	0.38	64
Pantanal	2.40e-01	2.68e-05	0.5	0.09	52

other biomes (Table 1), supporting our findings.

It is noticeable that the increase of SIF between 2015 and 2018 (Fig. 2 and 3) is also associated with the increase in rainfall for the same period (Fig. 4). The Amazon presented the lowest SIF changes related to rainfall and this biome has always enough precipitation to keep plant's water demands, even during droughts in the regions. This is consistent with what was reported previously, that in tropical ecosystems, the semi-arid biome has a higher sensitivity compared to the forest formations (Besnard et al., 2021; Allen et al., 2017).

In general, vegetation indices (e.g., NDVI, EVI, and SIF) in drier locations are more responsive to precipitation than in wet locations (Vicente-Serrano, 2006; Quiring and Ganesh, 2010; Li et al., 2018; Jiao et al., 2019; Green et al., 2020). This could be related to the root system, since the root system of a forest is deeper given to the forests a stronger resilience to short periods without precipitation, and not limiting the photosynthesis and SIF signal consequently (Barbosa et al., 2015; Jiao et al., 2019; Green et al., 2020; Uribe et al., 2021). In longer periods, this could be impacted because soil water is quite dependent on rainfall to restore its levels, and this could lead to changes in the sensitiveness of

forest ecosystems (Allen et al., 2019; Marca-Zevallos et al., 2022; Papastefanou et al., 2022).

In this sense, Shekhar et al. (2020) reported the drought impacts on SIF in different vegetations (using OCO-2 SIF) in the year 2018 for the European continent. They observed that crops were mostly affected by water deficits while forests presented resilience. Forest formations favor microclimate and have higher rates of rainfall, implying in a more water abundant system from atmosphere to soil, hence, even when some short periods of drought happen, this ecosystem is more resilient to these changes, being less sensitive to rainfall variations when compared to crops. This is in accordance with our results as agricultural systems considered in that study are similar to the typical cover found in Caatinga, Pampa, and Cerrado, the 03 most sensitive biomes of SIF with rainfall, in contrast to the Atlantic Forest and the Amazon biome in our study.

Additionally, forest age and height play an important role in photosynthesis regulation. Previous work shows that the SIF in the oldest and tallest trees in the forest has less sensitivity to precipitation variability due to the root system and the canopy structure (Giardina et al., 2018). This could also be related to the structural complexity of the vegetation cover in this biome, since less structured plants have more probability of SIF signal escape from the chlorophyll and can be more sensitive to environmental changes (Pinagé et al., 2022; van der Tol et al., 2019; Köhler et al., 2018). This is consistent with our findings, showing that the Amazon, a more canopy structured and rooted biome, has less sensitiveness to precipitation than Caatinga, a less canopy structured and rooted biome.

Another example of the importance that rainfall plays in the SIF variability was observed in ATF, PMP, and PNT biomes in the year 2017. The higher SIF averages could be explained by the increase in rainfall that year. Pantanal, which is a peculiar case, despite the annual increase in SIF with rainfall, presented the lower (and non-significant) SIF sensitivity to rainfall, probably due to the fact that this is a biome that has a flooded area most of the year (Zappi et al., 2015; Frankenberg

et al., 2014; Frankenberg and Berry, 2018).

#### 4.3. Implications

As presented in this work, SIF can capture the phytogeographic characteristics of major ecosystems, presenting rates that follow the typical limits and vegetation patterns. Given these same characteristics, these ecosystems have different responses to rainfall. Forest formations have a complex canopy than shrubs formations and this could lead to different signal sensitiveness, where less complex vegetation has more probability of SIF signal being emitted, hence being more sensitive to environmental changes (Pinagé et al., 2022; Giardina et al., 2018; Mohammed et al., 2019; Köhler et al., 2018).

The Amazon in recent years has been suffering from deforestation and wildfires (Aragão et al., 2018; Silveira et al., 2022), and this contributes to the desertification of this biome (Fernandez et al., 2019; Vieira et al., 2021; Mahari et al., 2020; Peng et al., 2020) and changes the forest structure (Silva Junior et al., 2020) that will imply in a less complex canopy structure and possibly a more sensitive SIF signal to environmental drivers (Pinagé et al., 2022; Besnard et al., 2021; Uribe et al., 2021; Köhler et al., 2018; Giardina et al., 2018), such as rainfall. Given this, one way of monitoring this change is to observe the sensitivity to precipitation, which could indicate the state of the forest, as it would be expected that in less structured vegetation SIF is more sensitive to changes in precipitation.

### 5. Conclusions

The spatial distribution of high-resolution SIF and its relation to rainfall across biomes allowed us to characterize the phytobiognomies of natural and contrasting ecosystems. The Amazon biome, which is a dense rainforest, presented higher SIF values with lower sensitivity to rainfall precipitation. On the other hand, Caatinga, which is a semi-arid biome, is the ecosystem where lower SIF averages were found but with a higher sensitivity to rainfall. Cerrado, Pampa, and the Atlantic Forest were closer in terms of SIF characteristics as they concentrate most of the agricultural lands of Brazil, with some spots of higher SIF values in the Atlantic Forest region where forest fragments still exist.

Differences in how SIF relates to rainfall point to contrasting impacts of climate change on those biomes, as in tropics rainfall precipitations Caatinga was the most sensitive, while the Amazon biome was the least. This difference is related to canopy complexity and structure since the probability of SIF escape from the leaf is lower with the increase of the complexity of vegetation. This could point out the impacts of climate change on these biomes, especially when deforestation advances in the Amazon, changing the vegetation structure and, as consequence, the sensitivity to climate conditions.

The importance of future studies exploring the gaps left behind this work needs to be emphasized. As our analysis focuses on interannual variability, the seasonal changes in SIF distribution and the relations for instance, with land use change and occupation, could be better explored to access the impact of anthropogenic activities in natural forest and crops photosynthesis and gross primary production.

#### Credit author statement

Conceptualization: L.M.C, N.L.S, A.R.P.; Formal analysis: L.M.C., J.R. S.C.M, G.C.M.; Methodology: L.M.C, A.R.P, N.L.S, G.C.M, J.R.S.C.M, R. C.; Data curation: L.M.C, G.A.A.S, J.R.S.C.M; Writing - original draft: L. M.C, N.L.S, G.C.M, G.A.A.S.; Writing - review and editing: All co-authors.

#### Funding

São Paulo Research Foundation (FAPESP) [Grants number: 2019/25,812–4 and 2021/06477–0], CNPq - National Council for Scientific

and Technological Development [Grant: 304075/2018–3 and 311981/2020–8], and the Coordenação de Aperfeiçoamento de Pessoal de Nível Superior – Brasil (CAPES) – Finance Code 001.

#### Declaration of competing interest

The authors declare that they have no known competing financial interests or personal relationships that could have appeared to influence the work reported in this paper.

#### Data availability

The data and code used in this work are available at [github](#)

#### Acknowledgments

We gratefully acknowledge the Brazilian São Paulo Research Foundation (FAPESP) [Grants number: 2019/25812–4 and 2021/06477–0], CNPq - National Council for Scientific and Technological Development [Grant: 304075/2018–3 and 311981/2020–8], and the Coordenação de Aperfeiçoamento de Pessoal de Nível Superior – Brasil (CAPES) – Finance Code 001. Also, authors are grateful to the open data provided by the NASA repositories.

#### Appendix A. Supplementary data

Supplementary data to this article can be found online at <https://doi.org/10.1016/j.envres.2022.114991>.

#### References

- Ainsworth, E.A., Long, S.P., 2005. What have we learned from 15 years of free-air CO<sub>2</sub> enrichment (FACE)? A meta-analytic review of the responses of photosynthesis, canopy properties and plant production to rising CO<sub>2</sub>. *New Phytol.* 165, 351–371. <https://doi.org/10.1111/j.1469-8137.2004.01224.x>
- Albright, R., Corbett, A., Jiang, X., Creecy, E., Newman, S., Li, K.F., Liang, M.C., Yung, Y. L., 2022. Seasonal variations of solar-induced fluorescence, precipitation, and carbon dioxide over the Amazon. *Earth Space Sci.* 9 (1), e2021EA002078 <https://doi.org/10.1029/2021EA002078>.
- Allen, K., Dupuy, J.M., Gei, M.G., Hulshof, C., Medvigi, D., Pizano, C., Salgado-Negret, B., Smith, C.M., Trierweiler, A., Van Bloem, S.J., Waring, B.G., Xu, X., Powers, J.S., 2017. Will seasonally dry tropical forests be sensitive or resistant to future changes in rainfall regimes? *Environ. Res. Lett.* 12 (2), 023001 <https://doi.org/10.1088/1748-9326/AA5968>.
- Allen, S.T., Kirchner, J.W., Braun, S., Siegwolf, R.T.W., Goldsmith, G.R., 2019. Seasonal origins of soil water used by trees. *Hydrol. Earth Syst. Sci.* 23 (2), 1199–1210. <https://doi.org/10.5194/HESS-23-1199-2019>.
- Alvares, C.A., Stape, J.L., Sentelhas, P.C., De Moraes Gonçalves, J.L., Sparovek, G., 2013. Köppen's climate classification map for Brazil. *Meteorol. Z.* 22 (6), 711–728. <https://doi.org/10.1127/0941-2948/2013/0507>.
- Anderegg, W.R.L., Trugman, A.T., Badgley, G., Anderson, C.M., Bartuska, A., Ciais, P., Cullender, D., Field, C.B., Freeman, J., Goetz, S.J., Hicke, J.A., Huntzinger, D., Jackson, R.B., Nickerson, J., Pacala, S., Randerson, J.T., 2020. Climate-driven risks to the climate mitigation potential of forests. *Science* 368 (6497). <https://doi.org/10.1126/SCIENCE.AAZ7005>.
- Aragão, L.E.O.C., Anderson, L.O., Fonseca, M.G., Rosan, T.M., Vedovato, L.B., Wagner, F. H., Silva, C.V.J., Silva Junior, C.H.L., Arai, E., Aguiar, A.P., Barlow, J., Berenguer, E., Deeter, M.N., Domingues, L.G., Gatti, L., Gloor, M., Malhi, Y., Marengo, J.A., Miller, J.B., et al., 2018. 21st Century drought-related fires counteract the decline of Amazon deforestation carbon emissions. *Nat. Commun.* 9 (1), 1–12. <https://doi.org/10.1038/s41467-017-02771-y>, 2018 9:1.
- Aratijo Santos, G.A., Morais Filho, L.F.F., Meneses, K. C. de, Silva Junior, C. A. da, Rolim, G. de S., La Scala, N., 2022. Hot spots and anomalies of CO<sub>2</sub> over eastern Amazonia, Brazil: a time series from 2015 to 2018. *Environ. Res.* 215, 114379 <https://doi.org/10.1016/J.ENVRES.2022.114379>.
- Barbosa, H.A., Lakshmi Kumar, T.V., Silva, L.R.M., 2015. Recent trends in vegetation dynamics in the South America and their relationship to rainfall. *Nat. Hazards* 77, 883–899. <https://doi.org/10.1007/s11069-015-1635-8>.
- Barbosa, M.L.F., Delgado, R.C., Forsad de Andrade, C., Teodoro, P.E., Silva Junior, C.A., Wanderley, H.S., Capristo-Silva, G.F., 2021. Recent trends in the fire dynamics in Brazilian Legal Amazon: interaction between the ENSO phenomenon, climate and land use. *Environmental Development* 39, 100648. <https://doi.org/10.1016/J.ENDEV.2021.100648>.
- Besnard, S., Santoro, M., Cartus, O., Fan, N., Linscheid, N., Nair, R., Weber, U., Koiral, S., Carvalhais, N., 2021. Global sensitivities of forest carbon changes to environmental conditions. *Global Change Biol.* 27 (24), 6467–6483. <https://doi.org/10.1111/GCB.15877>.

- Bontempo, E., Dalagnol, R., Ponzoni, F., Valeriano, D., 2020. Adjustments to sif aid the interpretation of drought responses at the caatinga of Northeast Brazil. *Rem. Sens.* 12 (19), 1–29. <https://doi.org/10.3390/rs12193264>.
- Bordonal, R. de O., Carvalho, J.L.N., Lal, R., de Figueiredo, E.B., de Oliveira, B.G., La Scala, N., 2018. Sustainability of sugarcane production in Brazil. A review. *Agron. Sustain. Dev.* 38 (2), 1–23. <https://doi.org/10.1007/S13593-018-0490-X>, 2018 38: 2.
- Câmara, I.G., 2003. Brief history of conservation in the Atlantic forest. In: Galindo-Leal, C., Câmara, I.G. (Eds.), *The Atlantic Forest of South America: Biodiversity Status, Threats, and Outlook*. Center for Applied Biodiversity Science e Island Press, Washington, D.C, pp. 31–42.
- Castro, A.O., Chen, J., Zang, C.S., Shekhar, A., Jimenez, J.C., Bhattacharjee, S., Kindu, M., Morales, V.H., Rammig, A., 2020. OCO-2 solar-induced chlorophyll fluorescence variability across ecoregions of the Amazon basin and the extreme drought effects of el nino (2015–2016). *Rem. Sens.* 12 (7), 1202. <https://doi.org/10.3390/rs12071202>.
- Celesti, M., van der Tol, C., Cogliati, S., Panigada, C., Yang, P., Pinto, F., Rascher, U., Miglietta, F., Colombo, R., Rossini, M., 2018. Exploring the physiological information of Sun-induced chlorophyll fluorescence through radiative transfer model inversion. *Rem. Sens. Environ.* 215, 97–108. <https://doi.org/10.1016/J.RSE.2018.05.013>.
- Cogliati, S., Celesti, M., Cesana, I., Miglietta, F., Genesio, L., Julitta, T., Schuettemeyer, D., Drusch, M., Rascher, U., Jurado, P., Colombo, R., 2019. A spectral fitting algorithm to retrieve the fluorescence spectrum from canopy radiance. *Rem. Sens.* 11 (16), 1840. <https://doi.org/10.3390/rs11161840>.
- Crisp, D., Fisher, B.M., O'dell, C., Frankenberg, C., Basilio, R., Bösch, H., Brown, L.R., Castano, R., Connor, B., Deutscher, N.M., Eldering, A., Griffith, D., Gunson, M., Kuze, A., Mandrake, L., McDuffie, J., Messerschmidt, J., Miller, C.E., Morino, I., Natraj, V., Notholt, J., O'Brien, D.M., Oyafuso, F., Polonsky, I., Robinson, J., Salawitch, R., Sherlock, V., Smyth, M., Suto, H., Taylor, T.E., Thompson, D.R., Wennberg, P.O., Wunch, D., Yung, Y.L., 2012. The ACOS CO<sub>2</sub> retrieval algorithm – Part II: global XCO<sub>2</sub> data characterization. *Atmos. Meas. Tech.* 5, 687–707. <https://doi.org/10.5194/amt-5-687-2012>.
- Crisp, D., Pollock, H., Rosenberg, R., Chapsky, L., Lee, R., Oyafuso, F., Frankenberg, C., Dell, C., Bruegge, C., Doran, G., Eldering, A., Fisher, B., Fu, D., Gunson, M., Mandrake, L., Osterman, G., Schwandner, F., Sun, K., Taylor, T., et al., 2017. The on-orbit performance of the Orbiting Carbon Observatory-2 (OCO-2) instrument and its radiometrically calibrated products. *Atmos. Meas. Tech.* 10 (1), 59–81. <https://doi.org/10.5194/AMT-10-59-2017>.
- Cui, Y., Chen, X., Gao, J., Yan, B., Tang, G., Hong, Y., 2018. Global water cycle and remote sensing big data: overview, challenge, and opportunities 2 (3), 282–297. <https://doi.org/10.1080/20964471.2018.1548052>.
- da Costa, L.M., de Araújo Santos, G.A., de Mendonça, G.C., Morais Filho, L.F.F., de Meneses, K.C., de Souza Rolim, G., La Scala, N., 2021. Spatiotemporal variability of atmospheric CO<sub>2</sub> concentration and controlling factors over sugarcane cultivation areas in southern Brazil. *Environ. Dev. Sustain.* 24 (4), 5694–5717. <https://doi.org/10.1007/S10668-021-01677-6>.
- da Costa, L.M., de Araújo Santos, G.A., Panosso, A.R., et al., 2022. An empirical model for estimating daily atmospheric column-averaged CO<sub>2</sub> concentration above São Paulo state, Brazil. *Carbon Bal. Manag.* 17, 9. <https://doi.org/10.1186/s13021-022-00209-7>.
- de Mendonça, G.C., Costa, R.C.A., Parras, R., de Oliveira, L.C.M., Abdo, M.T.V.N., Pacheco, F.A.L., Pisarra, T.C.T., 2022. Spatial indicator of priority areas for the implementation of agroforestry systems: an optimization strategy for agricultural landscapes restoration. *Sci. Total Environ.* 839, 156185 <https://doi.org/10.1016/J.SCITOTENV.2022.156185>.
- Doughty, R., Kurosu, T.P., Parazoo, N., Köhler, P., Wang, Y., Sun, Y., Frankenberg, C., 2022. Global GOSAT, OCO-2, and OCO-3 solar-induced chlorophyll fluorescence datasets. *Earth Syst. Sci. Data* 14, 1513–1529. <https://doi.org/10.5194/essd-14-1513-2022>.
- Du, E., de Vries, W., 2018. Nitrogen-induced new net primary production and carbon sequestration in global forests. *Environ. Pollut.* 242, 1476–1487. <https://doi.org/10.1016/J.JENVPOL.2018.08.041>.
- Duveiller, G., Cescatti, A., 2016. Spatially downscaling sun-induced chlorophyll fluorescence leads to an improved temporal correlation with gross primary productivity. *Rem. Sens. Environ.* 182, 72–89. <https://doi.org/10.1016/j.rse.2016.04.027>.
- Evert, R.F., Eichihirn, S.E., 2014. *Raven/Biologia Vegetal. 8<sup>a</sup> Edição*. Guanabara Koogan, Rio de Janeiro, pp. 278–316.
- Falahatkar, S., Mousavi, S.M., Farajzadeh, M., 2017. Spatial and temporal distribution of carbon dioxide gas using GOSAT data over Iran. *Environ. Monit. Assess.* 189 (12) <https://doi.org/10.1007/s10661-017-6285-8>.
- Fernandez, J.P.R., Franchito, S.H., Rao, V.B., 2019. Future changes in the aridity of South America from regional climate model projections. *Pure Appl. Geophys.* 176 (6), 2719–2728. <https://doi.org/10.1007/S00024-019-02108-4>.
- Frankenberg, C., Berry, J., 2018. Solar induced chlorophyll fluorescence: origins, relation to photosynthesis and retrieval. *Comprehensive Remote Sensing* 1–9, 143–162. <https://doi.org/10.1016/B978-0-12-409548-9.10632-3>.
- Frankenberg, C., O'Dell, C., Berry, J., Guanter, L., Joiner, J., Köhler, P., Pollock, R., Taylor, T.E., 2014. Prospects for chlorophyll fluorescence remote sensing from the Orbiting Carbon Observatory-2. *Rem. Sens. Environ.* 147, 1–12. <https://doi.org/10.1016/j.rse.2014.02.007>.
- Freitas, L.P.S., Lopes, M.L.M., Carvalho, L.B., Panosso, A.R., La Scala Júnior, N., Freitas, R.L.B., Minussi, C.R., Lotufo, A.D.P., 2018. Forecasting the spatiotemporal variability of soil CO<sub>2</sub> emissions in sugarcane areas in southeastern Brazil using artificial neural networks. *Environ. Monit. Assess.* 190 (12), 1–14. <https://doi.org/10.1007/s10661-018-7118-0>.
- Giardina, F., Konings, A.G., Kennedy, D., Alejomhammad, S.H., Oliveira, R.S., Uriarte, M., Gentile, P., 2018. Tall Amazonian forests are less sensitive to precipitation variability. *Nat. Geosci.* 11 (6), 405–409. <https://doi.org/10.1038/s41561-018-0133-5>, 2018 11:6.
- Gora, E.M., Esquivel-Muelbert, A., 2021. Implications of size-dependent tree mortality for tropical forest carbon dynamics. *Nature Plants* 7 (4), 384–391. <https://doi.org/10.1038/S41477-021-00879-0>.
- Green, J.K., Berry, J., Ciais, P., Zhang, Y., Gentile, P., 2020. Amazon rainforest photosynthesis increases in response to atmospheric dryness. *Sci. Adv.* 6 (47) <https://doi.org/10.1126/SCIADV.ABB7232>.
- Guan, K., Berry, J.A., Zhang, Y., Joiner, J., Guanter, L., Badgley, G., Lobell, D.B., 2016. Improving the monitoring of crop productivity using spaceborne solar-induced fluorescence. *Global Change Biol.* 22 (2), 716–726. <https://doi.org/10.1111/gcb.13136>.
- Guanter, L., Aben, I., Tol, P., Krijger, J.M., Hollenstein, A., Köhler, P., Damm, A., Joiner, J., Frankenberg, C., Landgraf, J., 2015. Potential of the TROPOMI onboard the Sentinel-5 Precursor for the monitoring of terrestrial chlorophyll fluorescence. *Atmos. Meas. Tech.* 8 (3), 1337–1352. <https://doi.org/10.5194/AMT-8-1337-2015>.
- Guanter, L., Bacour, C., Schneider, A., Aben, I., Van Kempen, T.A., Maignan, F., Retscher, C., Köhler, P., Frankenberg, C., Joiner, J., Zhang, Y., 2021. The TROPOSIF global sun-induced fluorescence dataset from the Sentinel-5P TROPOMI mission. *Earth Syst. Sci. Data* 13 (11), 5423–5440. <https://doi.org/10.5194/ESSD-13-5423-2021>.
- Hao, D., Asrar, G.R., Zeng, Y., Yang, X., Li, X., Xiao, J., Guan, K., Wen, J., Xiao, Q., Berry, J.A., Chen, M., 2021. Potential of hotspot solar-induced chlorophyll fluorescence for better tracking terrestrial photosynthesis. *Global Change Biol.* 27 (10), 2144–2158. <https://doi.org/10.1111/GCB.15554>.
- Heinrich, V.H.A., Dalagnol, R., Cassol, H.L.G., Rosan, T.M., de Almeida, C.T., Silva Junior, C.H.L., Campanharo, W.A., House, J.I., Sitch, S., Hales, T.C., Adami, M., Anderson, L.O., Aragão, L.E.O.C., 2021. Large carbon sink potential of secondary forests in the Brazilian Amazon to mitigate climate change. *Nat. Commun.* 12 (1), 1–11. <https://doi.org/10.1038/s41467-021-22050-1>, 2021 12:1.
- Huete, A., Didan, K., Miura, T., Rodriguez, E.P., Gao, X., Ferreira, L.G., 2002. Overview of the radiometric and biophysical performance of the MODIS vegetation indices, 2002. *Rem. Sens. Environ.* 83 (Issues 1–2), 195–213. [https://doi.org/10.1016/S0034-4257\(02\)00096-2](https://doi.org/10.1016/S0034-4257(02)00096-2). ISSN 0034-4257.
- INPE, 2008. Projeto PRODES: Monitoramento da floresta Amazônica Brasileira por satélite. Digital Database land classes of Amazon Region.
- Isaaks, E.H., Srivastava, R.M., 1989. *An Introduction to Applied Geostatistics*. Oxford University Press, New York, New York, US.
- Jiao, W., Chang, Q., Wang, L., 2019. The sensitivity of satellite solar-induced chlorophyll fluorescence to meteorological drought. *Earth's Future* 7 (5), 558–573. <https://doi.org/10.1029/2018EF001087>.
- Judd, W.S., Campbell, C.S., Stevens, P.F., Donoghue, M.J., 2009. *Sistemática vegetal: um enfoque filogenético*. Artmed, 3a. edição 632. Porto Alegre, RS.
- Köhler, P., Guanter, L., Kobayashi, H., Walther, S., Yang, W., 2018. Assessing the potential of sun-induced fluorescence and the canopy scattering coefficient to track large-scale vegetation dynamics in Amazon forests. *Rem. Sens. Environ.* 204, 769–785. <https://doi.org/10.1016/J.RSE.2017.09.025>.
- Li, X., Xiao, J., 2019. A global, 0.05-degree product of solar-induced chlorophyll fluorescence derived from OCO-2, MODIS, and reanalysis data. *Rem. Sens.* 11 (5), 517. <https://doi.org/10.3390/rs11050517>.
- Li, X., Xiao, J., He, B., 2018. Higher absorbed solar radiation partly offset the negative effects of water stress on the photosynthesis of Amazon forests during the 2015 drought. *Environ. Res. Lett.* 13 (4), 044005 <https://doi.org/10.1088/1748-9326/AABOB1>.
- Liang, S., Wang, D., He, T., Yu, Y., 2019. Remote sensing of earth's energy budget: synthesis and review 12 (7), 737–780. <https://doi.org/10.1080/17538947.2019.1597189>.
- Mahari, W.A.W., Azwar, E., Li, Y., Wang, Y., Peng, W., Ma, N.L., Yang, H., Rinklebe, J., Lam, S.S., Sonne, C., 2020. Deforestation of rainforests requires active use of UN's Sustainable Development Goals. *Sci. Total Environ.* 742, 140681 <https://doi.org/10.1016/J.SCITOTENV.2020.140681>.
- Marca-Zevallos, M.J., Moulletlet, G.M., Sousa, T.R., Schiatti, J., Coelho, L. de S., Ramos, J. F., Lima Filho, D. de A., Amaral, I.L., de Almeida Matos, F.D., Rincón, L.M., Cardenes Revilla, J.D., Pansonato, M.P., Gribel, R., Barbosa, E.M., Miranda, I.P. de A., Bonates, L.C. de M., Guevara, J.E., Salomão, R.P., Ferreira, L.V., et al., 2022. Local hydrological conditions influence tree diversity and composition across the Amazon basin. *Ecography* 2022 (11), e06125. <https://doi.org/10.1111/ECOG.06125>.
- Martini, D., Sakowska, K., Wohlfahrt, G., Pacheco-Labrador, J., van der Tol, C., Porcar-Castell, A., Magney, T.S., Carrara, A., Colombo, R., El-Madany, T.S., Gonzalez-Cascon, R., Martín, P., Julitta, T., Moreno, G., Rascher, U., Reichstein, M., Rossini, M., Migliavacca, M., 2022. Heatwave breaks down the linearity between sun-induced fluorescence and gross primary production. *New Phytol.* 233 (6), 2415–2428. <https://doi.org/10.1111/NPH.17920>.
- Merrick, T., Pau, S., Jorge, M.L.S.P., Silva, T.S.F., Bennartz, R., 2019. Spatiotemporal patterns and phenology of tropical vegetation solar-induced chlorophyll fluorescence across Brazilian biomes using satellite observations, 2019. *Rem. Sens.* 11 (15), 1746. <https://doi.org/10.3390/RS11151746>. Page 1746, 11.
- Mohammed, G.H., Colombo, R., Middleton, E.M., Rascher, U., van der Tol, C., Nedbal, L., Goulas, Y., Pérez-Priego, O., Damm, A., Meroni, M., Joiner, J., Cogliati, S., Verhoeef, W., Malenovský, Z., Gastellu-Etchegorry, J.P., Miller, J.R., Guanter, L., Moreno, J., Moya, I., et al., 2019. Remote sensing of solar-induced chlorophyll

- fluorescence (SIF) in vegetation: 50 years of progress. *Rem. Sens. Environ.* 231, 111177. <https://doi.org/10.1016/j.rse.2019.04.030>.
- Morais Filho, L.F.F., Meneses, K.C., de Santos, G.A. de A., Bicalho, E. da S., Rolim, G. de S., La Scala, N., 2021. xCO<sub>2</sub> temporal variability above Brazilian agroecosystems: a remote sensing approach. *J. Environ. Manag.* 288, 112433. <https://doi.org/10.1016/J.JENVMAN.2021.112433>.
- Morellato, L.P.C., Haddad, C.F.B., 2000. Introduction: the Brazilian atlantic forest. *Biotropica* 32, 786–792. <https://doi.org/10.1111/j.1744-7429.2000.tb00618.x>.
- Myers, N., Mittermeier, R., Mittermeier, C., et al., 2000. Biodiversity hotspots for conservation priorities. *Nature* 403, 853–858. <https://doi.org/10.1038/35002501>.
- O'Dell, C.W., Connor, B., Bösch, H., O'Brien, D., Frankenber, C., Castano, R., Christi, M., Elderling, D., Fisher, B., Gunson, M., McDuffie, J., Miller, C.E., Natraji, V., Oyafuso, F., Polonsky, I., Smyth, M., Taylor, T., Toon, G.C., Wennberg, P.O., Wunch, D., 2012. The ACOS CO<sub>2</sub> retrieval algorithm – Part 1: description and validation against synthetic observations. *Atmos. Meas. Tech.* 5, 99–121. <https://doi.org/10.5194/amt-5-99-2012>, 2012.
- Odum, E.P., 1971. *Fundamentals of Ecology*. WB Saunders Co, Philadelphia, p. 574.
- Oliveira-Filho, A.T., Dexter, K.G., Pennington, R.T., Simon, M.F., Bueno, M.L., Neves, D. M., 2021. On the floristic identity of Amazonian vegetation types. *Biotropica* 53, 767–777. <https://doi.org/10.1111/btp.12932>.
- Panosso, A.R., Marques, J., Pereira, G.T., La Scala, N., 2009. Spatial and temporal variability of soil CO<sub>2</sub> emission in a sugarcane area under green and slash-and-burn managements. *Soil Tillage Res.* 105 (2), 275–282. <https://doi.org/10.1016/j.still.2009.09.008>.
- Papastefanou, P., Zang, C.S., Angelov, Z., De Castro, A.A., Jimenez, J.C., De Rezende, L.F. C., Ruscica, R.C., Sakschewski, B., Sörensson, A.A., Thonicke, K., Vera, C., Viovy, N., Von Randow, C., Rammig, A., 2022. Recent extreme drought events in the Amazon rainforest: assessment of different precipitation and evapotranspiration datasets and drought indicators. *Biogeosciences* 19 (16), 3843–3861. <https://doi.org/10.5194/bg-19-3843-2022>.
- Parazoo, N.C., Bowman, K., Frankenber, C., Lee, J.E., Fisher, J.B., Worden, J., Jones, D. B.A., Berry, J., Collatz, G.J., Baker, I.T., Jung, M., Liu, J., Osterman, G., O'Dell, C., Sparks, A., Butz, A., Guerlet, S., Yoshida, Y., Chen, H., Gerbig, C., 2013. Interpreting seasonal changes in the carbon balance of southern Amazonia using measurements of XCO<sub>2</sub> and chlorophyll fluorescence from GOSAT. *Geophys. Res. Lett.* 40 (11), 2829–2833. <https://doi.org/10.1002/GRL.50452>.
- Paredes-Trejo, F., Barbosa, H., dos Santos, C.A.C., 2019. Evaluation of the performance of SM2RAIN-derived rainfall products over Brazil. *Rem. Sens.* 11 (9), 1113. <https://doi.org/10.3390/rs11091113>.
- Parras, R., de Mendonça, G.C., Costa, R.C.A., Pissarra, T.C.T., Valera, C.A., Fernandes, L. F.S., Pacheco, F.A.L., 2020. The configuration of forest cover in Ribeirão Preto: a diagnosis of Brazil's forest code implementation. *Sustain. Times* 12. <https://doi.org/10.3390/su12145686>.
- Peng, W., Sonne, C., Lam, S.S., Ok, Y.S., Alstrup, A.K.O., 2020. The ongoing cut-down of the Amazon rainforest threatens the climate and requires global tree planting projects: a short review. *Environ. Res.* 181, 108887. <https://doi.org/10.1016/J.ENVRES.2019.108887>.
- Pinagé, E.R., M. Bell, D., Longo, M., Gao, S., Keller, M., Silva, C.A., Ometto, J.P., Köhler, P., Frankenber, C., Huete, A., 2022. Forest structure and solar-induced fluorescence across intact and degraded forests in the Amazon. *Rem. Sens. Environ.* 274, 112998. <https://doi.org/10.1016/J.RSE.2022.112998>.
- Qiu, R., Li, X., Han, G., Xiao, J., Ma, X., Gong, W., 2022. Monitoring drought impacts on crop productivity of the U.S. Midwest with solar-induced fluorescence: GOSIF outperforms GOME-2 SIF and MODIS NDVI, EVI, and NIRV. *Agric. For. Meteorol.* 323, 109038. <https://doi.org/10.1016/J.AGRFORMAT.2022.109038>.
- Quiring, S.M., Ganesh, S., 2010. Evaluating the utility of the Vegetation Condition Index (VCI) for monitoring meteorological drought in Texas. *Agric. For. Meteorol.* 150 (3), 330–339. <https://doi.org/10.1016/J.AGRFORMAT.2009.11.015>.
- Raha, D., Dar, J.A., Pandey, P.K., Lone, P.A., Verma, S., Khare, P.K., Khan, M.L., 2020. Variation in tree biomass and carbon stocks in three tropical dry deciduous forest types of Madhya Pradesh 11 (2), 109–120. <https://doi.org/10.1080/17583004.2020.1712181>. India.
- Romero, J.M., Cordon, G.B., Lagorico, M.G., 2020. Re-absorption and scattering of chlorophyll fluorescence in canopies: a revised approach. *Rem. Sens. Environ.* 246, 111860. <https://doi.org/10.1016/J.RSE.2020.111860>.
- Salunkhe, O., Khare, P.K., Kumar, R., Khan, M.L., 2018. A systematic review on the aboveground biomass and carbon stocks of Indian forest ecosystems. *Ecological Processes* 7 (1), 1–12. <https://doi.org/10.1186/S13717-018-0130-Z>.
- Santos, R. de O., Delgado, R.C., Vilanova, R.S., Santana, R. O. de, Andrade, C. F. de, Teodoro, P.E., Silva Junior, C.A., Capristo-Silva, G.F., Lima, M., 2021. NMDI application for monitoring different vegetation covers in the Atlantic Forest biome, Brazil. *Weather Clim. Extrem.* 33, 100329. <https://doi.org/10.1016/J.WACE.2021.100329>.
- Shekhar, A., Chen, J., Bhattacharjee, S., Buras, A., Castro, A.O., Zang, C.S., Rammig, A., 2020. Capturing the impact of the 2018 European drought and heat across different vegetation types using OCO-2 solar-induced fluorescence. *Rem. Sens.* 12 (19), 3249. <https://doi.org/10.3390/RS12193249>, 2020, Vol. 12, Page 3249.
- Siabi, Z., Falahatkar, S., Alavi, S.J., 2019. Spatial distribution of XCO<sub>2</sub> using OCO-2 data in growing seasons. *J. Environ. Manag.* 244, 110–118. <https://doi.org/10.1016/j.jenvman.2019.05.049>.
- Siegmann, B., Cendrero-Mateo, M.P., Cogliati, S., Damm, A., Gamon, J., Herrera, D., Jedmowski, C., Junker-Frohn, L.V., Kraska, T., Muller, O., Rademske, P., van der Tol, C., Quiros-Vargas, J., Yang, P., Rascher, U., 2021. Downscaling of far-red solar-induced chlorophyll fluorescence of different crops from canopy to leaf level using a diurnal data set acquired by the airborne imaging spectrometer HyPlant. *Rem. Sens. Environ.* 264, 112609. <https://doi.org/10.1016/J.RSE.2021.112609>.
- Silva Junior, C.A., Lima, M., 2018. Soy moratorium in mato grosso: deforestation undermines the agreement. *Land Use Pol.* 71, 540–542. <https://doi.org/10.1016/J.LANDUSEPOL.2017.11.011>.
- Silva Junior, C.H.L., Aragão, L.E.O.C., Anderson, L.O., Fonseca, M.G., Shimabukuro, Y.E., Vancutsem, C., Achard, F., Beuchle, R., Numata, I., Silva, C.A., Maeda, E.E., Longo, M., Saatchi, S.S., 2020. Persistent collapse of biomass in Amazonian forest edges following deforestation leads to unaccounted carbon losses. *Sci. Adv.* 6 (40) <https://doi.org/10.1126/SCIAADV.AAZ8360>.
- Silva, D.V.S., Cruz, C.B.M., 2018. Tipologias da Caatinga: Uma Revisão em Apoio a Mapeamentos Através de Sensoriamento Remoto Orbital e GEORIA. *Revista Do Departamento De Geografia* 35, 113–120. <https://doi.org/10.11606/rdg.v35i0.142710>.
- Silveira, M.V.F., Silva-Junior, C.H.L., Anderson, L.O., Aragão, L.E.O.C., 2022. Amazon fires in the 21st century: the year of 2020 in evidence. *Global Ecol. Biogeogr.* <https://doi.org/10.1111/GEB.13577>.
- Sos Mata Atlântica & INPE, 2017. *Atlas dos remanescentes florestais da Mata Atlântica período 2015–2016*. São Paulo, Brasil. Fundação SOS Mata Atlântica. Instituto Nacional das Pesquisas Espaciais.
- Stackhouse, P.W., Westberg, D., Chandler, W.S., Zhang, T., Hoell, J.M., 2015. *Prediction of Worldwide Energy Resource (POWER) Agroclimatology Methodology*. NASA Langley Research Center. May 30, version 1.1. 0.
- Sun, X., Wang, M., Li, G., Wang, J., Fan, Z., 2020. Divergent sensitivities of spaceborne solar-induced chlorophyll fluorescence to drought among different seasons and regions. *ISPRS Int. J. Geo-Inf.* 9 (9), 542. <https://doi.org/10.3390/ijgi9090542>. MDPI AG.
- Sun, Y., Frankenber, C., Jung, M., Joiner, J., Guanter, L., Köhler, P., Magney, T., 2018. Overview of solar-induced chlorophyll fluorescence (SIF) from the orbiting carbon observatory-2: retrieval, cross-mission comparison, and global monitoring for GPP. *Rem. Sens. Environ.* 209, 808–823. <https://doi.org/10.1016/j.rse.2018.02.016>.
- Tadić, J.M., Qiu, X., Miller, S., Michalak, A.M., 2017. Spatio-temporal approach to moving window block kriging of satellite data v1.0. *Geosci. Model Dev. (GMD)* 10 (2), 709–720. <https://doi.org/10.5194/gmd-10-709-2017>.
- Tadić, J.M., Qiu, X., Yadav, V., Michalak, A.M., 2015. Mapping of satellite Earth observations using moving window block kriging. *Geosci. Model Dev. (GMD)* 8 (10), 3311–3319. <https://doi.org/10.5194/gmd-8-3311-2015>.
- Tagliabue, G., Panigada, C., Dechant, B., Baret, F., Cogliati, S., Colombo, R., Migliavacca, M., Rademsk, P., Schickling, A., Schütttemeyer, D., Verrelst, J., Rascher, U., Ryu, Y., Rossini, M., 2019. Exploring the spatial relationship between airborne-derived red and far-red sun-induced fluorescence and process-based GPP estimates in a forest ecosystem. *Rem. Sens. Environ.* 231, 111272. <https://doi.org/10.1016/J.RSE.2019.111272>.
- Terçariol, M.C., Brancaglioni, V.A., Júnior, J.P.A., Montanari, R., Teixeira Filho, M.C.M., Bolonhezi, A.C., et al., 2016. Spatial variability of soil co2 emission in soybean and sugarcane areas in mato grosso do sul cerrado, Brazil. *Journal of Geospatial Modelling* 2 (1), 45–66. <https://doi.org/10.22615/2526-1746-jgm-2.1-5888>.
- Tuomisto, H., Ruokolainen, K., Kalliola, R., Linna, A., Danjoy, W., Rodriguez, Z., 1995. Dissecting amazonian biodiversity. *Science* 269, 5220.63 (1995), pp. 63–66.
- Turner, A.J., Köhler, P., Magney, T.S., Frankenber, C., Fung, I., Cohen, R.C., 2021. Extreme events driving year-to-year differences in gross primary productivity across the US. *Biogeosciences* 18 (24), 6579–6588. <https://doi.org/10.5194/BG-18-6579-2021>.
- Uribé, M.R., Sierra, C.A., Dukes, J.S., 2021. Seasonality of tropical photosynthesis: a pantropical map of correlations with precipitation and radiation and comparison to model outputs. *J. Geophys. Res.: Biogeosciences* 126 (11), e2020JG006123. <https://doi.org/10.1029/2020JG006123>.
- van der Tol, C., Vilfan, N., Dauwe, D., Cendrero-Mateo, M.P., Yang, P., 2019. The scattering and re-absorption of red and near-infrared chlorophyll fluorescence in the models Fluspect and SCOPE. *Remote Sensing of Environment* 232, 111292. <https://doi.org/10.1016/J.RSE.2019.111292>.
- Vicente-Serrano, S.M., 2006. Evaluating the impact of drought using remote sensing in a mediterranean, semi-arid region. *Nat. Hazards* 40 (1). <https://doi.org/10.1007/S11069-006-0009-7>, 173–208 2006 40:1.
- Vieira, R.M.D.S.P., Tomasella, J., Barbosa, A.A., Martins, M.A., Rodriguez, D.A., Rezende, F.S.D., Carrillo, F., Santana, M.D.O., 2021. Desertification risk assessment in Northeast Brazil: current trends and future scenarios. *Land Degrad. Dev.* 32 (1), 224–240. <https://doi.org/10.1002/LDR.3681>.
- Xiao, J., Chevallier, F., Gomez, C., Guanter, L., Hicke, J.A., Huete, A.R., Ichii, K., Ni, W., Pang, Y., Rahman, A.F., Sun, G., Yuan, W., Zhang, L., Zhang, X., 2019. Remote sensing of the terrestrial carbon cycle: a review of advances over 50 years. *Rem. Sens. Environ.* 233, 111383. <https://doi.org/10.1016/J.RSE.2019.111383>.
- Xu, X., Medvigy, D., Trugman, A.T., Guan, K., Good, S.P., Rodriguez-Iturbe, I., 2018. Tree cover shows strong sensitivity to precipitation variability across the global tropics. *Global Ecol. Biogeogr.* 27 (4), 450–460. <https://doi.org/10.1111/GBE.12707>.
- Yang, Y., Zhu, J., Zhao, C., Liu, S., Tong, X., 2011. The spatial continuity study of NDVI based on Kriging and BPNN algorithm. *Math. Comput. Model.* 54 (3), 1138–1144. <https://doi.org/10.1016/j.mcm.2010.11.046>.
- Yu, L., Wen, J., Chang, C.Y., Frankenber, C., Sun, Y., 2019a. High-resolution global contiguous SIF of OCO-2. *Geophys. Res. Lett.* 46 (3), 1449–1458. <https://doi.org/10.1029/2018GL081109>.

- Yu, L., Wen, J., Chang, C.Y., Frankenberg, C., Sun, Y., 2019b. High Resolution Global Contiguous SIF Estimates Derived from OCO-2 SIF and MODIS. ORNL Distributed Active Archive Center. <https://doi.org/10.3334/ORNLDaac/1696>.
- Zappi, D.C., Ranzato Filardi, F.L., Leitman, P., Souza, V.C., Walter, B.M.T., Pirani, J.R., Morim, M.P., Queiroz, L.P., Cavalcanti, T.B., Mansano, V.F., Forzza, R.C., Abreu, M.C., Acevedo-Rodríguez, P., Agra, M.F., Almeida, E.B., Almeida, G.S.S., Almeida, R.F., Alves, F.M., Alves, M., et al., 2015. Growing knowledge: an overview of Seed Plant diversity in Brazil. *Rodriguesia* 66 (4), 1085–1113. <https://doi.org/10.1590/2175-7860201566411>.
- Zhang, Y., Joiner, J., Hamed Aleommahmmed, S., Zhou, S., Gentine, P., 2018. A global spatially contiguous solar-induced fluorescence (CSIF) dataset using neural networks. *Biogeosciences* 15 (19), 5779–5800. <https://doi.org/10.5194/bg-15-5779-2018>.